Geophysical Research Letters

RESEARCH LETTER
10.1029/2024GL113826

Role of Synthetic Biofilms in Bed Evolution and the Formation of Sedimentary Structures

Willian R. Assis[1,2], **Lian Shen**[1,3], **and Judy Q. Yang**[1,2]

[1]St. Anthony Falls Laboratory, University of Minnesota Twin Cities, Minneapolis, MN, USA, [2]Department of Civil, Environmental, and Geo Engineering, University of Minnesota Twin Cities, Minneapolis, MN, USA, [3]Department of Mechanical Engineering, University of Minnesota Twin Cities, Minneapolis, MN, USA

Key Points:

- Typical microbial sedimentary structures were observed on the sediment bed covered by synthetic biofilms
- Biofilms can reduce bed roughness by an order of magnitude
- Biofilm-sediment interactions lead to the formation of multi-scale geometries of bedforms with locally elevated bedform features

Supporting Information:

Supporting Information may be found in the online version of this article.

Correspondence to:

J. Q. Yang,
judyyang@umn.edu

Citation:

Assis, W. R., Shen, L., & Yang, J. Q. (2025). Role of synthetic biofilms in bed evolution and the formation of sedimentary structures. *Geophysical Research Letters*, *52*, e2024GL113826. https://doi.org/10.1029/2024GL113826

Received 25 NOV 2024
Accepted 5 FEB 2025

Author Contributions:

Conceptualization: Willian R. Assis, Judy Q. Yang
Data curation: Willian R. Assis, Judy Q. Yang
Formal analysis: Willian R. Assis
Funding acquisition: Lian Shen, Judy Q. Yang
Investigation: Willian R. Assis
Methodology: Willian R. Assis, Judy Q. Yang
Project administration: Judy Q. Yang
Resources: Judy Q. Yang
Software: Willian R. Assis
Supervision: Judy Q. Yang
Validation: Willian R. Assis, Judy Q. Yang
Visualization: Willian R. Assis

Abstract Microbes are known to shape topographies; however, mechanisms of biofilm-sediment interactions and the dynamic evolution of biofilm-covered bedforms remain poorly understood. Here, we explore the effects of synthetic biofilms on the geometry and temporal evolution of underwater bedforms through flume experiments. Our results demonstrate that synthetic biofilms can produce sedimentary structures similar to those formed by natural microbes, including wrinkles, pits, flip-overs, roll-ups, mat chips, and erosional edges. We observed the formation of wrinkles, a common geological feature, due to the accumulation of sand grains on the biofilms. Furthermore, we demonstrated that biofilms can reduce bed roughness by an order of magnitude in the low flow regime. However, the subsequent biofilm-sediment interactions can increase local bedform size, forming multi-scale geometries of bedforms. Our study improves the fundamental understanding of the landscape dynamics of bedforms covered by natural biofilms.

Plain Language Summary Microbes, such as algae and bacteria, are known to modify landscapes through sediment stabilization, nutrient cycling, and the formation of sedimentary structures. Sediments covered by microbial layers, referred to as biofilms, have been found in various environments, including streams, coastal zones, and other shallow water ecosystems. However, our understanding of the role of biofilms in shaping landscapes remains scarce due to a lack of systematically controlled experiments. To address this research gap, we conducted experiments in a water channel and monitored the evolution of a bed covered by synthetic biofilms. We observed the formation of sedimentary structures that are similar to microbially induced sedimentary structures found in geological records and those observed on sediments covered by natural biofilms. Our experiments suggest that while the initial biofilms can reduce bed roughness by up to an order of magnitude, biofilm fragments can contribute to the formation of multi-scale geometries of bedforms by locally increasing bed height due to their interaction and aggregation with sediments. Our results provide direct observational data on how biofilms impact the time evolution and shape of bed topographies, offering a foundation for predictions of bedforms and landscapes in the presence of microbial layers.

1. Introduction

Biofilms, consisting of microorganisms enclosed in extracellular polymeric substances (EPS), are found in a variety of aquatic environments, including sediment surfaces in deep oceans, granular systems at the bottom of rivers, and mudflat ecosystems (Depetris et al., 2022; Ericksson et al., 2004; Fagherazzi et al., 2017; Gerdes, 2007). These microbial communities grow mainly in wet and moist environments, being found as mats or films, and are one of the most spread life found on Earth (Ehrlich & Newman, 2008; Flemming et al., 2016; Reid et al., 2000). The interaction of biofilms with flow and sediment can affect sediment erosion, contaminant transport, and the dynamics and propagation of bedforms (Gerbersdorf et al., 2020). Additionally, microorganisms could have potentially played an important role in shaping the Martian surface, leading to biosignatures that could possibly explain the emergence of life (Noffke, 2010; Vago et al., 2017; Westall et al., 2015). Despite the importance of biofilms in Earth surface processes, a fundamental understanding of the mechanisms underlying these impacts remains lacking.

Biofilms impact sediment transport and bed topography through two ways. First, when interacting with granular systems, biofilms can create a biological cohesion among grains by producing EPS, which functions as a glue that bonds particles together and hinders their free movement (Fang et al., 2017; Gu et al., 2020; Neumann et al., 1970). This process causes sediments to stick together and erode as micro-aggregates (Flemming &

Writing – original draft: Willian R. Assis, Judy Q. Yang
Writing – review & editing: Willian R. Assis, Lian Shen, Judy Q. Yang

Wingender, 2010; Hagadorn & Mcdowell, 2012; Hu et al., 2003; Piqué et al., 2016; Vignaga et al., 2013). Second, microorganisms can form membranes or carpet-like mats on the surface of the sediment bed (Andersen et al., 2010; Dade et al., 1990; Stal, 2010; Yallop et al., 1994), providing shelters for the underneath grains until the mats are detached or peeled off from the bed. Although many studies have explored the role of biological cohesion in sediment bed topography (Malarkey et al., 2015; Parsons et al., 2016), the influence of mat-like biofilms on the temporal evolution of sediment bed remains under-investigated.

The term "biofilm" refers for microbial cells encased in EPS on surfaces, typically with a thickness on the scale of millimeters. The term "microbial mat" is used when the biofilms form thicker, mat-like layers, on the scale of centimeters to decimeters, on the unbounded sediment surfaces (Cuadrado, 2020; Maisano et al., 2019). In the present study, the term "biofilm" refers to the thick cohesive films on the sediment surface (Cuadrado, 2020). Biofilms and microbial mats in aquatic ecosystems have been associated with the formation of various sedimentary structures, such as wrinkles, pits, small-scale ripples, and other surface textures on rocks and sand beds, respectively (Gerdes et al., 2000; Stal, 2012; Vignale et al., 2021). The formation of the Microbially Induced Sedimentary Structures (MISS) is still being debated, and their shapes are controlled by several factors, including mat thickness, grain sizes, flow conditions, and sources of formation (Cuadrado & Pan, 2018; Davies et al., 2016; Hagadorn & Bottjer, 1997; Maisano et al., 2019; Noffke et al., 2001, 2006; Thomas et al., 2013). Among the various types of sedimentary structures, wrinkles (pits or ridges on the order of millimeters or centimeters) have been a focus of many studies due to their origin and modes of formation (Porada & Bouougri, 2007). Some theories suggest that wrinkles could form beneath buried microbial mats (Hagadorn & Bottjer, 1999) or result from mat deformation induced by shear stresses (Bouougri & Porada, 2002). In contrast, Mariotti et al. (2014) observed the formation of wrinkles in a wave flume due to the movement of mat fragments under bed shear stress below the critical shear stress of the sand. A key challenge in the theories explaining submerged wrinkles lies in understanding how grains organize into ridges and pits, while simultaneously ensuring that no erosion of the mat occurs. Despite the ongoing debates and many different theories regarding the origin of these structures, experimental evidence about their formation remains limited, making it challenging to validate existing theories or propose alternative formation processes.

Laboratory investigations in recent years have provided valuable insights into the important role of biofilms in sediment transport, yet a fundamental understanding of the dynamic interactions between biofilms and sediment remains incomplete. Experiments were performed in two main ways: by mixing synthetic EPS such as Xanthan gun with sand (C. Chen et al., 2020; X. Chen et al., 2023; Malarkey et al., 2015; Parsons et al., 2016; Tolhurst et al., 2002; Xuewu et al., 1996), or by cultivating biofilms with microbe-inoculated sand (Droppo et al., 2001; Gibbs, 1983; Hagadorn & Mcdowell, 2012; Piqué et al., 2016). Using the former approach, Malarkey et al. (2015) investigated bedform development with varying amounts of EPS (ratio of dry sand to dry Xanthan powder). The authors showed that low concentrations of EPS within sediments can increase the time of bedform development by up to two orders of magnitude. Similarly, Parsons et al. (2016) demonstrated that biological cohesion, formed by the presence of EPS matrix, has a greater effect on the bedform development compared to physical cohesion, which is caused by mud or clay. While this approach (mixing uniformly EPS with sand) simulates the effect of biofilm-induced cohesion among sediment grains, they do not simulate the mat-like biofilm layers on the surface of sediment bed. In the second approach, Hagadorn and Mcdowell (2012) studied the effect of microbial layers on the sediment surface during the genesis of bedforms. They showed that mats thicker than 1 mm cause the grains to transport in the form of aggregates and observed the flip-over, roll-up, and rip-up structures resulting from interactions between sand and biofilms. In addition, they showed that grains around 3–5 mm below the sediment surface have much less microbial communities than grains at the surface. Even though the authors explored the initial phase of the biofilm formation–where a film or mat is formed on the sediment surface–the processes of sedimentation and deposition of microbial layers can present colonized sediments underneath the surface, leading to more complex interactions (Cuadrado, 2020). While the studies with natural biofilms reproduced sedimentary structures resembling those found in geological records (Hagadorn & Mcdowell, 2012), detailed quantitative measurements of the temporal evolution of the bedforms remain lacking. A fundamental understanding of the temporal evolution of biofilm-impacted topography is critical because the interactions between the biofilms and sediments are dynamic processes, and the mechanisms underlying the formation of bedforms influenced by biofilms remains unclear. To the authors' knowledge, few if any studies have investigated how biofilms (which may modify the active and underlying layers of the sediment bed) can affect the temporal evolution of bedforms

while simultaneously producing sedimentary structures similar to those observed in microbially induced structures within geological records.

This study aims to investigate the effect of biofilms on the temporal evolution of bedforms through flume experiments. By creating a synthetic biofilm and applying it to the sediment bed, we examine the influence of biofilms on bedform generation, the interactions between biofilm fragments and sediments, and the role of these interactions in shaping bedform structures. Our results elucidate the mechanisms by which biofilms impact the bedforms evolution, providing a method to study the evolution of ancient strata inside laboratory, and laying a foundation for future prediction of bedforms covered by natural microbial layers.

2. Materials and Methods

Experiments were conducted in the tilting sediment-recirculating flume that is 15.0 m long, 0.92 m wide, and 0.65 m deep at Saint Anthony Falls Laboratory (SAFL) at the University of Minnesota, Twin Cities. Water flow was controlled by a hydraulic valve, and flow rate was determined by a calibration curve. We used a fixed tailgate of 26 cm located downstream of the channel to maintain a minimum flow depth (Martin & Jerolmack, 2013). In addition, in downstream of the bed, we placed a 13 cm wall to maintain a minimum depth of sediments in the flume. The initial condition for all tests was a flatbed composed of silica particles of median grain size of $d_{50} = 0.45$ mm and density of $\rho_s = 2650$ kg/m^3. The flow discharge (Q) ranged from 171.3 to 219.9 m^3/hr to generate different sizes of bedforms (ripple-like to dune-like shape, which we will call here low and high flow regimes, respectively). The water depth (h) varied from 0.16 to 0.20 m, and the bulk flow velocity $U = Q/Bh$ ranged from 0.29 to 0.37 m/s, where B is the channel width. The shear velocity u_* ranged from 0.02 to 0.07 m/s, and it was obtained by the mean momentum equation in uniform flow, $u_* = \sqrt{gR_hS_w}$, where $g = 9.81$ m/s^2 is the gravitational acceleration, $R_h = Bh/B + 2h$ is the hydraulic radius, and S_w is the slope of water-free surface. We set the flume at slopes of 0 and 0.2° to achieve the low and high flow regimes, respectively. The test section was 5 m long in the flume and started at 7 m from the inlet of water, which provided roughly a steady water surface slope. To minimize the disturbances on the flow in the inlet part of the channel, we used a mesh of cobbles, a matrix of pipes, and cardboard box located downstream of the head box (see Supporting Information S1 for the calibration curve, a layout of the experimental setup and all hydraulic parameters in each tested case).

The topography evolution was measured using a JSR Ultrasonic DPR300 Pulser/Receiver with transducer frequencies ranging from 1 to 2.25 MHz. The sonar system can record bed elevation with millimeter accuracy, and we set to acquire bed topography every 1 cm during each swath. We scanned the center line of the channel while the transducer was submerged roughly 1 cm below the water surface, to avoid any disturbance in the flow related to the measurements. The elevation of water was taken using a MassaSonic M-500/220 ultrasonic probe set to measure it every 1 cm as well. The topography and water elevation were recorded in CSV files. MatLab and Python codes were written to post-process the data. For the data processing, we used the same approach presented in Lee et al. (2021, 2022). The bed profiles were decomposed into small- and large-scale bedforms using the Fast Fourier Transform (FFT) with low- and high-pass filters, respectively. The cut-off lengths used to separate different scales of bedforms were based on the 95th percentile of bedform lengths in the unfiltered data. We quantified the evolution of the mean steepness of the bed $\left(\overline{H/L}\right)$, which is the ratio of the mean height $\left(\overline{H}\right)$ to the mean length $\left(\overline{L}\right)$, and the mean bed roughness $\left(\overline{K_s}\right)$ for each swath, in accordance with Lee et al. (2021). The bed roughness $\overline{K_s} = 25\overline{H}^2/\overline{L}$ was determined based on Van Rijn (1984) and Parsons et al. (2016).

To create synthetic biofilms, we mixed Xanthan gum (Catalog Number: 32096 from Chem-Impex company) with water, and we created a gel of 5% (weight ratio of Xanthan powder to water). This gel resembles the biofilms found near the surface regions (C. Chen et al., 2019), which have EPS ranging from ∼1% to ∼5% (dry weight) in freshwater and intertidal muds, respectively (Gerbersdorf et al., 2009; Malarkey et al., 2015; Taylor & Paterson, 1998). The gel can form a mat-like structure similar to the biofilms cultivated using natural microbes (Hagadorn & Mcdowell, 2012; Piqué et al., 2016), and the amount added to the sediments was based on the volume of sand in the flume once the abiotic bedforms reached a steady-state condition. This procedure provided a biofilm thickness of roughly 4 mm. Once the solution was prepared, we waited 24 hr before applying it over the wet sediments, and another 24 hr before starting the experiment. We selected this range of time to prepare and apply the gel-like material over the bed to ensure better adhesion to the sediments and to minimize any possible evaporation that could occur in the biopolymer when exposed to air for longer periods (C. Chen et al., 2020;

Fagherazzi et al., 2017; Vignaga et al., 2012). If the gel were left to sit much longer, it could dry out and develop cracks, making it unsuitable to simulate biofilms in fully saturated conditions. In order to compare the gel with biofilms, we measured the peak tensile stress on the material using MTS LSB 102D equipment with a load cell of 100 N. The peak stress found was 3333 ± 444 Pa and the results were within the range presented by previous works (Vignaga et al., 2012). Finally, we measured the rheology properties of the synthetic mat using a DHR 5333-0056 rheometer (see Supporting Information S1 for photos of the initial mat thickness, information about the initial conditions, and all measured data presented in this manuscript).

3. Results

3.1. Biofilm-Induced Sedimentary Structures

After running water through the channel above the sediment bed covered with synthetic biofilm, we observed structures including flip-overs, roll-ups, wrinkles, mat chips, pits, and erosional edges, as shown in Figure 1a–1f. Our observations were similar to the microbially induced sedimentary structures found in Western Australia (Figures 1g, 1h, 1k, and 1l from Noffke et al. (2013)), sandstones (Figure 1i from Sarkar et al. (2016)), and rock records (Figure 1j from Mariotti et al. (2014)). The formation of flip-overs occurred primarily at the beginning of the experiments, when the flow caused the mat to tear and bend (Figure 1a). Subsequently, mat fragments and roll-up structures occurred when biofilms started rolling and curling up, aggregating with sand and other mat parts (Figure 1b).

From Figures 1a and 1b, we note that the process of peeling off the biofilm was not homogeneous throughout the flume, causing fractions of biofilms to aggregate with other film or sand parts. This effect increases the thickness of the biofilm in some parts of the channel, making it more resistant to erosion. As a result of the heterogeneity of the biofilms, some parts were eroded during the flow, while other parts got trapped in the sediments. These trapped fragments were later buried by the sand moving from upstream, generating layered sedimentary structures (see Supporting Information S1 for a photo taken from a frozen sand below the sediment surface showing the buried biofilm). Our experiments further suggest that the buried biofilm fragments can trap sediment moving above them, generating irregular wrinkle-like structures (Figures 1c and 2d).

In addition to wrinkles, pits were observed as a result of the detachment of buried mat from the bed (Figure 1d). We also noted the presence of pits and wrinkles on the same bed. Furthermore, Figure 1e shows the presence of mat chips, which are segments of the biofilm that were broken from the mat and integrated with sand. Finally, Figure 1f presents erosional edges, slightly higher surfaces due to erosion of a large part of the mat. The similarity between the structures generated using synthetic biofilms and those observed in geological records, as well as in previous studies using natural microbes, indicates that the synthetic mats we created effectively replicated the role of biofilms in bedform formation. In contrast to natural biofilms, which can take months to develop in large scale experiments, synthetic biofilms provide a rapid and alternative method for investigating the effect of microbial layers on bed topography under various hydrodynamic conditions.

3.2. Genesis of Bedforms

To investigate the bed evolution, we recorded the formation of bedforms with and without synthetic biofilms. Figure 2 shows the bed evolution for both abiotic and biofilm-bound sediments during low and high flow regimes. In the abiotic scenario, the bedforms reached a steady state condition within 5–10 hr, remaining roughly the same morphology obtained in the last panels of Figures 2a and 2c, with ripple and dune-like shapes for low and high flow regimes, respectively. In addition to time lapse images, we scanned the topography using acoustic echosounders and computed the spatio-temporal evolution of the bed for abiotic sand (Figures 3a and 3b) and biofilm-covered sand (Figures 3c and 3d) under both the low and high flow conditions.

In the low flow regime (u_* in the range of 0.02–0.03 m/s; see Supporting Information S1 for all hydraulic parameters), the spatially averaged steepness and roughness of abiotic sediment bed increased over the first 8 hr, and then remained roughly constant at 0.04 and 13.51 mm (Figures 3e and 3g), respectively. In contrast, for biofilm-covered sediment, the bed steepness and roughness increased in the first 2 hr due to biofilm erosion, before reaching a plateau. At this plateau, the bed steepness in the biotic case was 0.01, four times smaller than the case without biofilms, while the bed roughness was 2.00 mm, an order of magnitude smaller than the value for abiotic sand. Similarly, in high flow regime (u_* in the range of 0.07 m/s), the steepness and roughness of abiotic bed

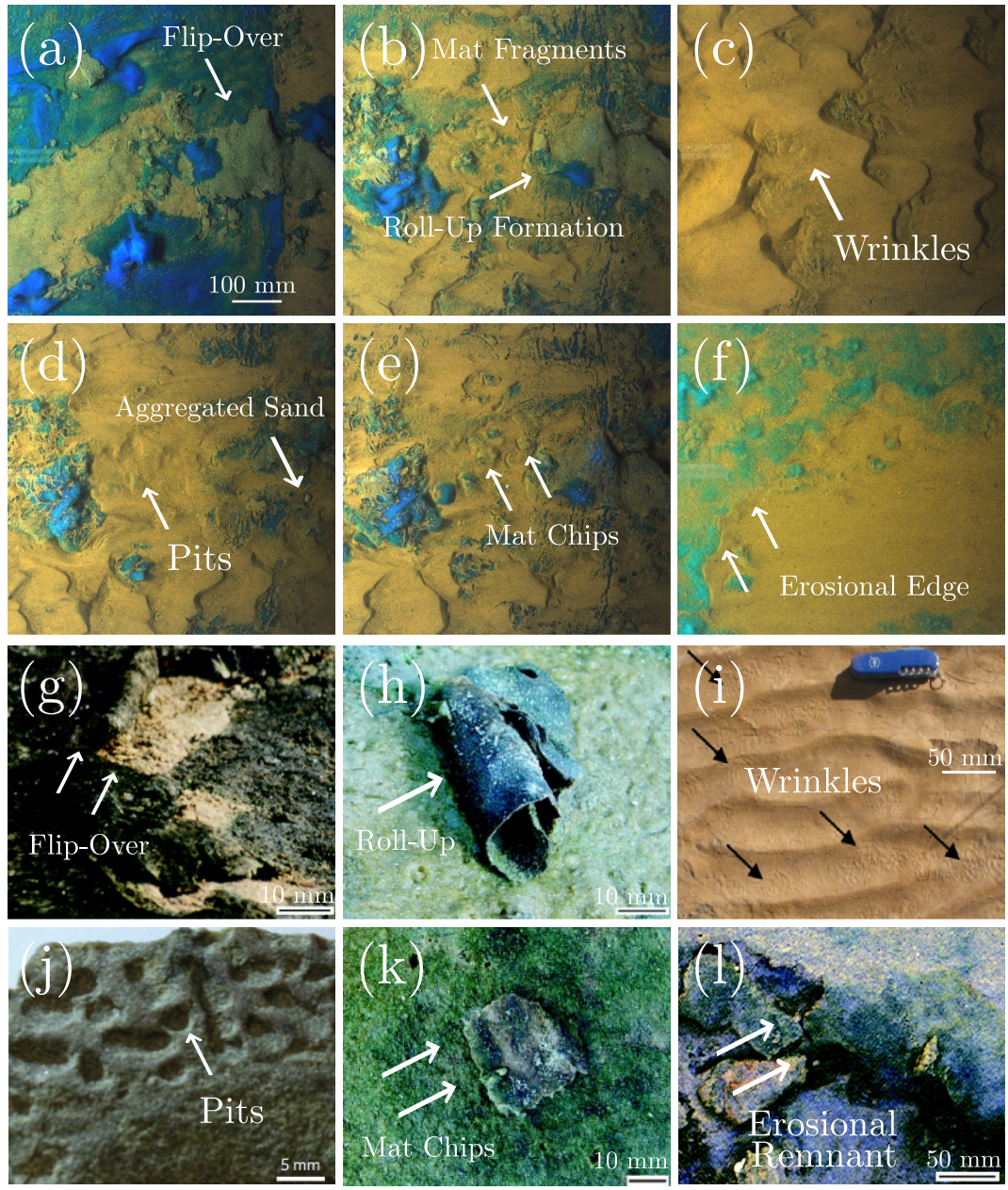

Figure 1. Snapshots showing sedimentary structures on the bed due to synthetic biofilms (a–f), and microbially induced sedimentary structures due to natural microbial mats (g–l). Flip-over (a, g), roll-up (b, h), wrinkles (c, i), pits (d, j), mat chips (e, k), and erosional edges (f, l). Figures (g, h, k, l) were located in Western Australia and were extracted and modified from Noffke et al. (2013). Figures (i, j) were extracted and modified from Sarkar et al. (2016) and Mariotti et al. (2014), respectively.

reached 0.04 and 25.84 mm, while the biofilm condition reduced these values to 0.03 and 14.30 mm (Figures 3f and 3h), respectively. Our study first confirms the role of biofilms in suppressing the initial formation of bedforms and further suggests that this effect depends on the bed shear stress or flow rate and thickness of the microbial layers on the sediment surface (Hagadorn & Mcdowell, 2012).

3.3. Multi-Scale Bedforms Induced by Biofilm-Sediment Interactions

During our experiments, abiotic bedforms reached their equilibrium shape within the 5–10 hr from the beginning of the experiments, remaining in the steady condition afterward (Figures 3e–3h). However, for biofilm-covered

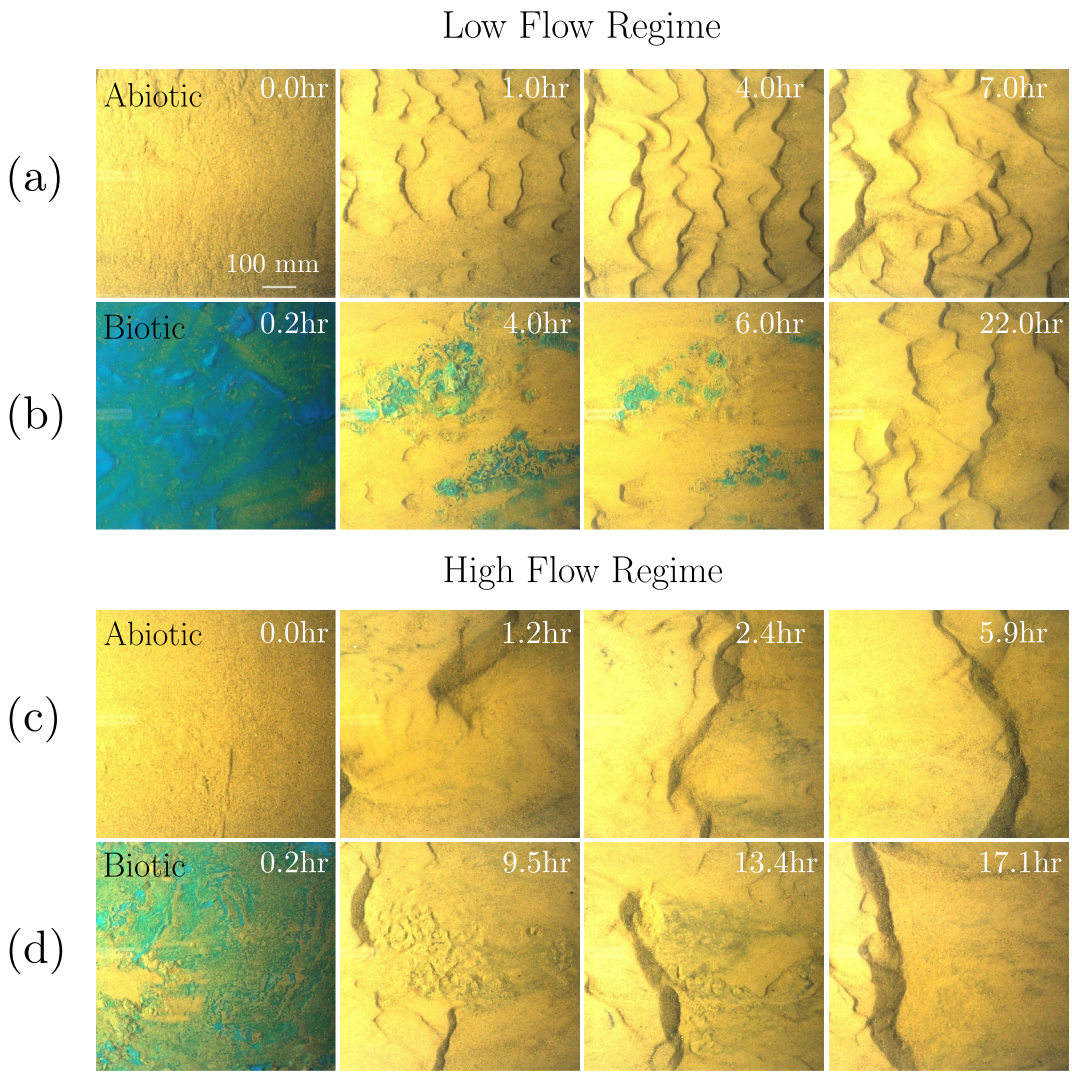

Figure 2. Figures (a, b) show the bed evolution in abiotic and biotic cases during the low flow discharge, while figures (c, d) illustrate bed development in the high flow regime for the same cases. The flow is from left to right in all images. Note that the times are different in each row.

sediment, we observed subsequent changes in bed topography due to the dynamic interactions between sand and buried biofilms after 15 hr. As presented in Section 3.1, part of the biofilms was buried during the process of erosion. This buried biofilm can create wrinkle-like structures due to the accumulation of sand over the irregular buried film, as well as change the bedforms size and migration beyond the early stage (time less than 15 hr). To capture this effect, we measured the spatio-temporal evolution for the biofilm-sand condition in low and high flow regimes, as shown in Figures 4a and 4b (the dashed lines are set on 15 hr in each figure), respectively.

In the low flow regime, we observed the formation of chunks of sand, resulting from aggregation of buried biofilms and moving sediments. The clumps of sediment lead to the formation of locally elevated bedforms, as shown by the red fronts in Figure 4a. These locally elevated bedform features resulted in bedforms with multi-scale heights and wavelengths (Figures 4a and 4c). However, it was not observed in the high flow regime (Figure 4b), as the flow condition was strong enough to break the aggregation. Figures 4c and d present topography along the center line of the channel at the instants of 15 and 30 hr for abiotic and biofilm conditions in the low flow regime, and 15 and 45 hr for the same conditions in the high flow regime, respectively. For the biofilm-covered beds in the low flow regime (Figure 4c), we observe the presence of a larger bedform with the wavelength and height on the order of 1 m and 40 mm, respectively, while small bedforms located downstream exhibit wavelengths and heights on the order of 10 mm and 0.1 m. We included in the Supporting Information S1

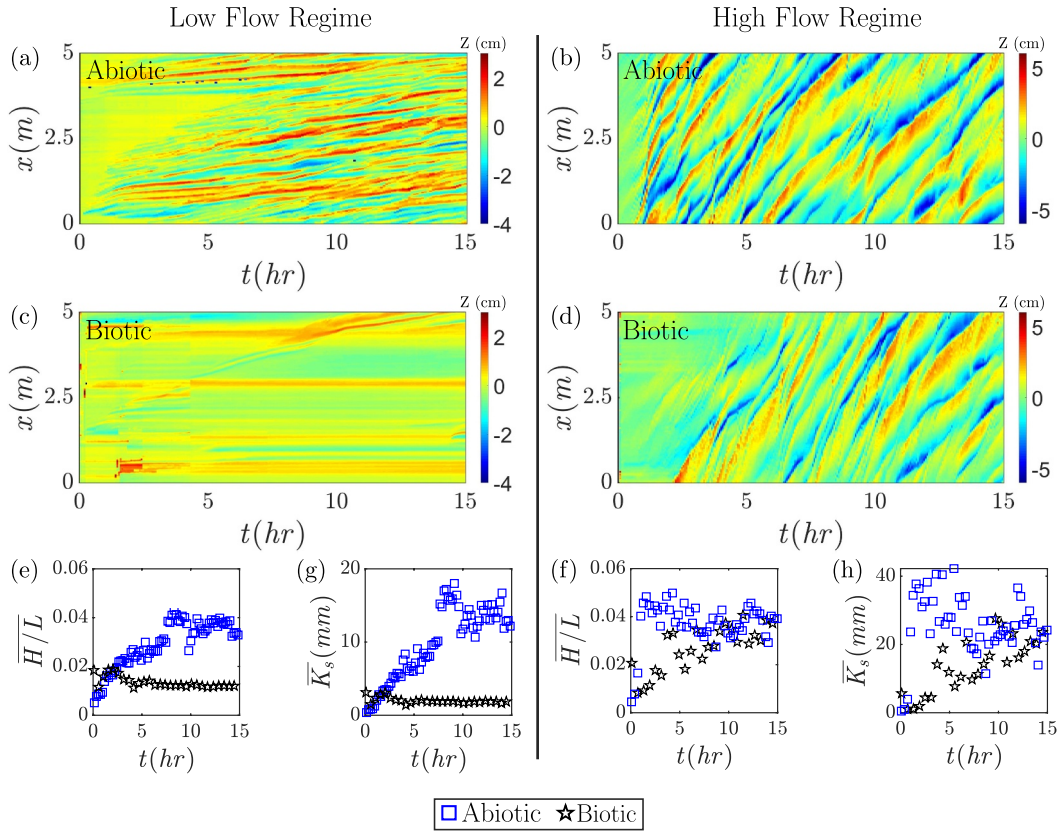

Figure 3. Figures (a, c) show the spatio-temporal evolution of abiotic and biofilm-covered beds in the low flow regime, while Figures (b, d) show the cases in the high flow regime. Figures (e, f) show the evolution of the spatially averaged steepness, while (g, h) present the spatially averaged bed roughness for abiotic and biotic scenarios during low and high flow discharges, respectively.

snapshots of bedforms over a biofilm layer, a test case where we imposed a patch of biofilms, and profiles of the bedforms over time. The observation of multi-scale bedforms due to biofilms, to our knowledge, has rarely been discussed in previous studies.

To further investigate the distribution of bedform sizes, we analyzed the morphology (heights and lengths) and dynamics (celerities) using HPF (High-Pass Filter, subscript h) and LPF (Low-Pass Filter, subscript l) filters based on the probability density functions (PDFs). The analysis using high and low pass filters allows us to identify two distinct spatial signals, decoupling the signals into fast and small bedforms (HPF) along with slow and large bedforms (LPF) (Lee et al., 2021). The data presented in Figures 4e–4g is from the low flow regime experiment (see Supporting Information S1 for the high flow regime data), as no significant changes were observed once we imposed higher shear velocity. We analyzed the data from 15 hr onwards, as the biofilms had already eroded at that time, and compared it with the steady-state condition for abiotic sand (last 5 hr of the Figures 3a and 3b). Compared with abiotic sand, which has mean values of $H_h = 14.68$ mm and $H_l = 15.79$ mm at the plateau state (from 10 to 15 hr), the H_h and H_l for biofilm-covered sand are 12.12 and 14.40 mm at 15 hr onward (Figure 4e). This difference suggests that buried biofilms decreased the height of small-scale bedforms (HPF) due to the presence of EPS on the bed and the trapping of sediments on the surface mat.

The mean values of the length distributions of HPF and LPF were 0.16 and 0.44 m for abiotic sand, while biofilm-covered sand reached values of 0.19 and 0.63 m, respectively (Figure 4f). It suggests that biofilms increased the wavelengths of bedforms (HPF) due to the trapping of sediments on the surface mat, and also increased the length of large-scale bedforms (LPF) due to sediment aggregation (see Figures S4 and S5 in Supporting Information S1 for a buried synthetic biofilm and for ripples crossing biofilm layers, respectively). A similar trend is observed in the celerity (Figure 4g), where biofilm-covered small-scale bedforms presented slightly higher mean velocities ($U_h = 0.07$ mm/s) compared with abiotic sand ($U_h = 0.05$ mm/s). Compared with the decrease in the size of

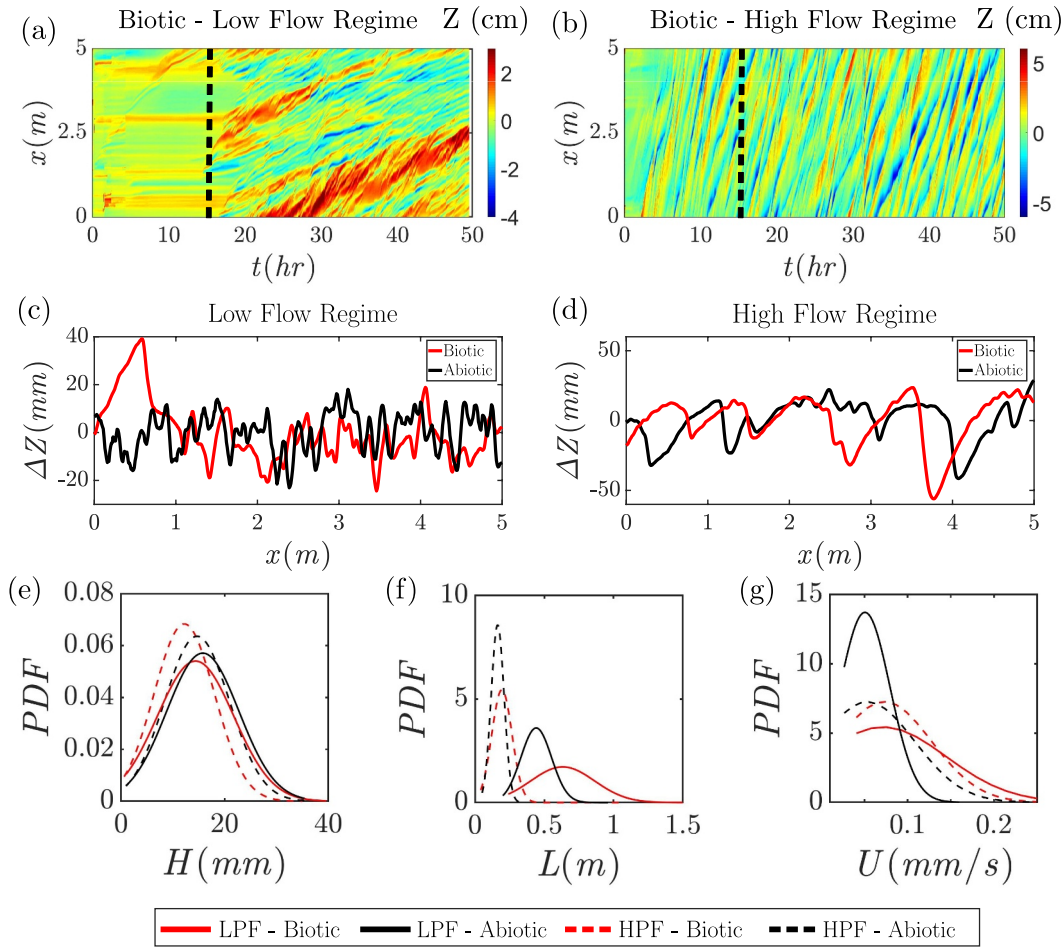

Figure 4. Figures (a, b) show the spatio-temporal evolution of biofilm-covered beds for low and high flow discharges (the dashed lines are set to 15 hr). Figures (c, d) present topography along the center line of the channel comparing the biofilm-bound condition with the abiotic cases for low and high flow regimes, respectively. Figures (e, f, g) show PDFs of bedforms heights, lengths and celerities using HPF and LPF for low discharge, respectively.

bedforms composed of cohesive materials (EPS or clay in Malarkey et al. (2015) and Parsons et al. (2016)), our results show that the interactions between biofilms and sand can increase the bed size due to the agglomeration of sediments by buried biofilms, leading to the formation of multi-scale geometries of bedforms.

4. Discussion

The flip-overs, roll-ups, mat chips, and erosional edges observed in our study are similar to those documented in the field by Maisano et al. (2019, 2023), and in the laboratory experiments with natural microorganisms (Hagadorn & Mcdowell, 2012). Additionally, we observed eroding and burying processes of synthetic biofilms over time, consistent with the observations by Schieber (2007) using natural microbial mats. Moreover, we noticed the formation of irregular wrinkle-like structures caused by buried biofilm fragments trapping sand moving above them. This wrinkle formation mechanism, due to the differential movement of biofilm and sediment layers, resembles the mechanisms of adhesion ripples in air, where dry sand grains adhere to a wet surface (Kocurek & Fielder, 1982). The biofilm-induced wrinkles (Hagadorn & Bottjer, 1997) have some similarities with the modern wrinkle patterns described in Porada and Bouougri (2007). Similarly, wrinkles have also been observed when a layer of sand moved over mud in intertidal regions (Allen, 1984), consistent with our observation that the differential movement of two layers of materials can generate wrinkle structures. While the wrinkle-like structures are due to the differential movement of biofilm and sediment layers in our experiments, more regular reticulate patterns were formed by cyanobacteria on the top of microbial mats after a storm, as

documented in a field study by Cuadrado and Pan (2018). In addition, mat fragments have been shown to shape sand surface generating wrinkle-like structures in a wave tank when the fluid flow is below the threshold of sediment transport (Mariotti et al., 2014).

During the genesis of bedforms, we observed that biofilms can suppress entirely the formation of the bed, specially during the low flow regimes (u_* in the range of 0.02–0.03 m/s). Our results show that the imposed shear velocity could break the biofilm layer (forming the sedimentary structures presented in Figure 1), but it was not strong enough to form bedforms during the initial stages of evolution. It is important to note that the experimental replicates provide similar sedimentary structures as shown in Figure 1 with consistent genesis of bedforms within the initial 15 hr (Figure S12 in Supporting Information S1). In Figure S13a in Supporting Information S1, bedforms appeared around 20 hr from the start of the experiment. In contrast, in Figure 4a, bedforms appeared around 15–16 hr from the beginning of the experiments. This small variation is likely due to the heterogeneity of biofilms and flows across different cases. The effect of suppressing bed formation in the high flow regime (u_* in the range of in the range of 0.07 m/s) is smaller than in the low flow regime, likely because the stronger shear velocity can more easily disrupt the biofilm layers and form bedforms afterward. Different from our laboratory study (which we investigated the genesis of bedforms and not the initiation of sedimentary structures), field works, such as Maisano et al. (2019, 2023), explored the MISS formation during seawater floodings, showing that slow currents (0.5 m/s as velocity), can rip mat fragments from the underlying sediments, while severe storms (1.6 m/s as velocity) could tear the superficial cohesive microbial mat, creating large roll-up structures over long distances in the tidal flat. These studies corroborate with our laboratory method, which shows that sedimentary structures could be formed under high and low hydrodynamic conditions, but the bedform formation is more prominent during the high flow discharge when in the presence of biofilms.

Lastly, the interaction between biofilms and sediments can lead to the formation of multi-scale geometries of bedforms by locally increasing bed height due to biofilm-sediment aggregation. When compared with field works, biofilm-induced elevated bedforms have been observed in nature, as described in the book of Davis and Dalrymple (2012), particularly in Figure 10.17j, where ripple surface is covered by an elevated sand patch stabilized by diatoms. Additionally, we showed that biofilm-sediment interactions can decrease the height of small-scale bedforms (HPF) due to the presence of EPS on the bed and the trapping of sediments on the surface mat. In accordance with our study, Cuadrado (2020) presented field observations on ripple bed development in a tidal flat. The author provided evidence that floods currents can cause sediment transport across the microbial mats, forming several types of ripples. Moreover, the detached microbial mats could form folds, resulting in very small biostabilized ripples on their surface, where the formation of these ripples occurred due to the accumulation of sand on the microbial mats. Although our experiments show that using synthetic biofilms can produce sedimentary structures resembling those in geological records, we acknowledge that natural environments may present more dynamic conditions—such as floods, seasonal variations, biofilm patches, and microbial recolonization in sediments—potentially leading to more complex outcomes.

5. Conclusions

In the present study, we investigated the effects of sediments covered by microbial layers on the geometry and temporal evolution of bedforms through flume experiments using synthetic biofilms. We provide laboratory evidences that synthetic biofilms can reproduce sedimentary structures similar to those found in geological records attributed to natural microbes, such as pits, wrinkles, flip-overs, roll-ups, mat chips, and erosional edges. Our experiments show that at the early stage, biofilms can reduce the bed roughness by up to an order of magnitude, and this effect is more prominent in the low flow condition. However, once bedforms start to form, biofilms can generate locally elevated structures, forming multi-scale sizes of bedforms. Additionally, we observed the formation of wrinkles, a common feature in geological records, due to the accumulation of sediments on biofilms. Our results suggest that surficial biofilms play a critical role in bedforms evolution and geomorphology, and that in addition to reduce bedform sizes at the early stage, the subsequent interactions between sediments and buried biofilms can generate distinct structures and lead to a wider distribution of bedform sizes than abiotic sediment. Our synthetic biofilm method offers a possible way to investigate the complex biofilm-sediment interactions and provide insights into the role that microorganisms can play on bed evolution and the formation of sedimentary structures. Our results have applications in the prediction of coastal erosion, understanding of tidal flat sedimentology, and explanation of the potential formation of biosignatures on the Martian surface.

Data Availability Statement

Data supporting this work were generated by ourselves and are available in Assis and Yang (2024). The data also can be found in Supporting Information S1. The numerical scripts used to process the data were adapted and modified from Lee et al. (2021, 2022), and more details can be found in https://doi.org/10.13020/e1fe-sb56.

Acknowledgments
This study is supported by Office of Navy Research Grant N00014-23-1-2559 and National Science Foundation CAREER Award EAR-2236497. The authors would like to express their gratitude to the SAFL staff, specially Ben Erickson, Cheryl Miller, Jeff Marr, Matt Lueker, Erik Noren, Erik Steen, and Chris Milliren, for their support to our experiments. The authors are also grateful to Michele Guala and Chris Paola for helpful discussions, to Soukaina Benaich for the rheology measurements, to Isha Mutreja for the assistance in the tensile stress measurements, and to Diana Cuadrado and one anonymous reviewer for their valuable comments.

References

Allen, J. (1984). Wrinkle marks: An intertidal sedimentary structure due to aseismic soft-sediment loading. *Sedimentary Geology*, *41*(1), 75–95. https://doi.org/10.1016/0037-0738(84)90003-4

Andersen, T., Lanuru, M., Van Bernem, C., Pejrup, M., & Riethmueller, R. (2010). Erodibility of a mixed mudflat dominated by microphytobenthos and cerastoderma edule, East Frisian Wadden Sea, Germany. *Estuarine, Coastal and Shelf Science*, *87*(2), 197–206. https://doi.org/10.1016/j.ecss.2009.10.014

Assis, W. R., & Yang, J. (2024). Data supporting the manuscript role of microbial mats in bed evolution and the formation of sedimentary structures [Dataset][Software]. *Retrieved from the Data Repository for the University of Minnesota (DRUM)*. https://doi.org/10.13020/8tj0-xt19

Bouougri, E., & Porada, H. (2002). Mat-related sedimentary structures in neoproterozoic peritidal passive margin deposits of the West African craton (anti-atlas, Morocco). *Sedimentary Geology*, *153*(3–4), 85–106. https://doi.org/10.1016/s0037-0738(02)00103-3

Chen, C., Wu, L., & Harbottle, M. (2019). Influence of biopolymer gel-coated fibres on sand reinforcement as a model of plant root behaviour. *Plant and Soil*, *438*(1–2), 361–375. https://doi.org/10.1007/s11104-019-04033-w

Chen, C., Wu, L., & Harbottle, M. (2020). Exploring the effect of biopolymers in near-surface soils using xanthan gum–modified sand under shear. *Canadian Geotechnical Journal*, *57*(8), 1109–1118. https://doi.org/10.1139/cgj-2019-0284

Chen, X., Kang, Y., Zhang, Q., Jin, C., & Zhao, K. (2023). Biophysical contexture of coastal biofilm-sediments varies heterogeneously and seasonally at the centimeter scale across the bed-water interface. *Frontiers in Marine Science*, *10*, 1131543. https://doi.org/10.3389/fmars.2023.1131543

Cuadrado, D. G. (2020). Geobiological model of ripple genesis and preservation in a heterolithic sedimentary sequence for a supratidal area. *Sedimentology*, *67*(5), 2747–2763. https://doi.org/10.1111/sed.12718

Cuadrado, D. G., & Pan, J. (2018). Field observations on the evolution of reticulate patterns in microbial mats in a modern siliciclastic coastal environment. *Journal of Sedimentary Research*, *88*(1), 24–37. https://doi.org/10.2110/jsr.2017.79

Dade, W. B., Davis, J. D., Nichols, P. D., Nowell, A. R., Thistle, D., Trexler, M. B., & White, D. C. (1990). Effects of bacterial exopolymer adhesion on the entrainment of sand. *Geomicrobiology Journal*, *8*(1), 1–16. https://doi.org/10.1080/01490459009377874

Davies, N. S., Liu, A. G., Gibling, M. R., & Miller, R. F. (2016). Resolving miss conceptions and misconceptions: A geological approach to sedimentary surface textures generated by microbial and abiotic processes. *Earth-Science Reviews*, *154*, 210–246. https://doi.org/10.1016/j.earscirev.2016.01.005

Davis, R. A., & Dalrymple, R. W. (2012). *Principles of tidal sedimentology* (Vol. 625). Springer.

Depetris, A., Tagliavini, G., Peter, H., Kühl, M., Holzner, M., & Battin, T. J. (2022). Biophysical properties at patch scale shape the metabolism of biofilm landscapes. *npj Biofilms and Microbiomes*, *8*(1), 5. https://doi.org/10.1038/s41522-022-00269-0

Droppo, I., Lau, Y., & Mitchell, C. (2001). The effect of depositional history on contaminated bed sediment stability. *Science of the Total Environment*, *266*(1–3), 7–13. https://doi.org/10.1016/s0048-9697(00)00748-8

Ehrlich, H. L., & Newman, D. K. (2008). *Geomicrobiology*. CRC Press.

Ericksson, P., Altermann, W., Nelson, D., Mueller, W., & Catuneanu, O. (2004). *The Precambrian Earth: Tempos and events: Developments in precambrian geology*. Elsevier.

Fagherazzi, S., Viggato, T., Vieillard, A., Mariotti, G., & Fulweiler, R. (2017). The effect of evaporation on the erodibility of mudflats in a mesotidal estuary. *Estuarine, Coastal and Shelf Science*, *194*, 118–127. https://doi.org/10.1016/j.ecss.2017.06.011

Fang, H., Lai, H., Cheng, W., Huang, L., & He, G. (2017). Modeling sediment transport with an integrated view of the biofilm effects. *Water Resources Research*, *53*(9), 7536–7557. https://doi.org/10.1002/2017wr020628

Flemming, H.-C., & Wingender, J. (2010). The biofilm matrix. *Nature Reviews Microbiology*, *8*(9), 623–633. https://doi.org/10.1038/nrmicro2415

Flemming, H.-C., Wingender, J., Szewzyk, U., Steinberg, P., Rice, S. A., & Kjelleberg, S. (2016). Biofilms: An emergent form of bacterial life. *Nature Reviews Microbiology*, *14*(9), 563–575. https://doi.org/10.1038/nrmicro.2016.94

Gerbersdorf, S. U., Koca, K., de Beer, D., Chennu, A., Noss, C., Risse-Buhl, U., et al. (2020). Exploring flow-biofilm-sediment interactions: Assessment of Current status and future challenges. *Water Research*, *185*, 116182. https://doi.org/10.1016/j.watres.2020.116182

Gerbersdorf, S. U., Westrich, B., & Paterson, D. M. (2009). Microbial extracellular polymeric substances (EPS) in fresh water sediments. *Microbial Ecology*, *58*(2), 334–349. https://doi.org/10.1007/s00248-009-9498-8

Gerdes, G. (2007). Structures left by modern microbial mats in their host sediments. In *Atlas of microbial mat features preserved within the siliciclastic rock record* (p. 5).

Gerdes, G., Klenke, T., & Noffke, N. (2000). Microbial signatures in peritidal siliciclastic sediments: A catalogue. *Sedimentology*, *47*(2), 279–308. https://doi.org/10.1046/j.1365-3091.2000.00284.x

Gibbs, R. J. (1983). Effect of natural organic coatings on the coagulation of particles. *Environmental Science & Technology*, *17*(4), 237–240. https://doi.org/10.1021/es00110a011

Gu, Y., Zhang, Y., Qian, D., Tang, Y., Zhou, Y., & Zhu, D. Z. (2020). Effects of microbial activity on incipient motion and erosion of sediment. *Environmental Fluid Mechanics*, *20*(1), 175–188. https://doi.org/10.1007/s10652-019-09706-9

Hagadorn, J. W., & Bottjer, D. J. (1997). Wrinkle structures: Microbially mediated sedimentary structures common in subtidal siliciclastic settings at the proterozoic-phanerozoic transition. *Geology*, *25*(11), 1047–1050. https://doi.org/10.1130/0091-7613(1997)025<1047:wsmmss>2.3.co;2

Hagadorn, J. W., & Bottjer, D. J. (1999). Restriction of a late neoproterozoic biotope; suspect-microbial structures and trace fossils at the vendian-cambrian transition. *PALAIOS*, *14*(1), 73–85. https://doi.org/10.2307/3515362

Hagadorn, J. W., & Mcdowell, C. (2012). Microbial influence on erosion, grain transport and bedform genesis in sandy substrates under unidirectional flow. *Sedimentology*, *59*(3), 795–808. https://doi.org/10.1111/j.1365-3091.2011.01278.x

Hu, C., Liu, Y., Paulsen, B. S., Petersen, D., & Klaveness, D. (2003). Extracellular carbohydrate polymers from five desert soil algae with different cohesion in the stabilization of fine sand grain. *Carbohydrate Polymers*, *54*(1), 33–42. https://doi.org/10.1016/s0144-8617(03)00135-8

Kocurek, G., & Fielder, G. (1982). Adhesion structures. *Journal of Sedimentary Research*, *52*(4), 1229–1241.
Lee, J., Musa, M., & Guala, M. (2021). Scale-dependent bedform migration and deformation in the physical and spectral domains. *Journal of Geophysical Research: Earth Surface*, *126*(5), e2020JF005811. https://doi.org/10.1029/2020jf005811
Lee, J., Singh, A., & Guala, M. (2022). Reconstructing sediment transport by migrating bedforms in the physical and spectral domains. *Water Resources Research*, *58*(7), e2022WR031934. https://doi.org/10.1029/2022wr031934
Maisano, L., Cuadrado, D. G., & Gómez, E. A. (2019). Processes of miss-formation in a modern siliciclastic tidal flat, Patagonia (Argentina). *Sedimentary Geology*, *381*, 1–12. https://doi.org/10.1016/j.sedgeo.2018.12.002
Maisano, L., Quijada, I. E., Raniolo, L. A., & Cuadrado, D. G. (2023). Modification of large microbial mat deformation structures before burial: A modern case study. *Sedimentary Geology*, *447*, 106355. https://doi.org/10.1016/j.sedgeo.2023.106355
Malarkey, J., Baas, J. H., Hope, J. A., Aspden, R. J., Parsons, D. R., Peakall, J., et al. (2015). The pervasive role of biological cohesion in bedform development. *Nature Communications*, *6*(1), 6257. https://doi.org/10.1038/ncomms7257
Mariotti, G., Pruss, S., Perron, J., & Bosak, T. (2014). Microbial shaping of sedimentary wrinkle structures. *Nature Geoscience*, *7*(10), 736–740. https://doi.org/10.1038/ngeo2229
Martin, R. L., & Jerolmack, D. J. (2013). Origin of hysteresis in bed form response to unsteady flows. *Water Resources Research*, *49*(3), 1314–1333. https://doi.org/10.1002/wrcr.20093
Neumann, A. C., Gebelein, C. D., & Scoffin, T. P. (1970). The composition, structure and erodability of subtidal mats, abaco, Bahamas. *Journal of Sedimentary Research*, *40*(1).
Noffke, N. (2010). *Geobiology: Microbial mats in sandy deposits from the Archean era to today*. Springer Science & Business Media.
Noffke, N., Christian, D., Wacey, D., & Hazen, R. M. (2013). Microbially induced sedimentary structures recording an ancient ecosystem in the ca. 3.48 billion-year-old dresser formation, pilbara, Western Australia. *Astrobiology*, *13*(12), 1103–1124. https://doi.org/10.1089/ast.2013.1030
Noffke, N., Eriksson, K. A., Hazen, R. M., & Simpson, E. L. (2006). A new window into early archean life: Microbial mats in Earth's oldest siliciclastic tidal deposits (3.2 ga moodies group, South Africa). *Geology*, *34*(4), 253–256. https://doi.org/10.1130/g22246.1
Noffke, N., Gerdes, G., Klenke, T., & Krumbein, W. E. (2001). Microbially induced sedimentary structures: A new category within the classification of primary sedimentary structures. *Journal of Sedimentary Research*, *71*(5), 649–656. https://doi.org/10.1306/2dc4095d-0e47-11d7-8643000102c1865d
Parsons, D. R., Schindler, R. J., Hope, J. A., Malarkey, J., Baas, J. H., Peakall, J., et al. (2016). The role of biophysical cohesion on subaqueous bed form size. *Geophysical Research Letters*, *43*(4), 1566–1573. https://doi.org/10.1002/2016gl067667
Piqué, G., Vericat, D., Sabater, S., & Batalla, R. J. (2016). Effects of biofilm on river-bed scour. *Science of the Total Environment*, *572*, 1033–1046. https://doi.org/10.1016/j.scitotenv.2016.08.009
Porada, H., & Bouougri, E. H. (2007). Wrinkle structuresa critical review. *Earth-Science Reviews*, *81*(3–4), 199–215. https://doi.org/10.1016/j.earscirev.2006.12.001
Reid, R. P., Visscher, P. T., Decho, A. W., Stolz, J. F., Bebout, B., Dupraz, C., et al. (2000). The role of microbes in accretion, lamination and early lithification of modern marine stromatolites. *Nature*, *406*(6799), 989–992. https://doi.org/10.1038/35023158
Sarkar, S., Choudhuri, A., Mandal, S., & Eriksson, P. G. (2016). Microbial mat-related structures shared by both siliciclastic and carbonate formations. *Journal of Palaeogeography*, *5*(3), 278–291. https://doi.org/10.1016/j.jop.2016.05.001
Schieber, J. (2007). Flume experiments on the durability of sandy microbial mat fragments during transport. In *Atlas of microbial mat features preserved within the siliciclastic rock record* (p. 248).
Stal, L. J. (2010). Microphytobenthos as a biogeomorphological force in intertidal sediment stabilization. *Ecological Engineering*, *36*(2), 236–245. https://doi.org/10.1016/j.ecoleng.2008.12.032
Stal, L. J. (2012). Cyanobacterial mats and stromatolites. In *Ecology of cyanobacteria II: Their diversity in space and time* (pp. 65–125). Springer.
Taylor, I., & Paterson, D. (1998). Microspatial variation in carbohydrate concentrations with depth in the upper millimetres of intertidal cohesive sediments. *Estuarine, Coastal and Shelf Science*, *46*(3), 359–370. https://doi.org/10.1006/ecss.1997.0288
Thomas, K., Herminghaus, S., Porada, H., & Goehring, L. (2013). Formation of kinneyia via shear-induced instabilities in microbial mats. *Philosophical Transactions of the Royal Society A: Mathematical, Physical & Engineering Sciences*, *371*(2004), 20120362. https://doi.org/10.1098/rsta.2012.0362
Tolhurst, T., Gust, G., & Paterson, D. M. (2002). The influence of an extracellular polymeric substance (EPS) on cohesive sediment stability. In *Proceedings in Marine Science* (Vol. 5, pp. 409–425). Elsevier. https://doi.org/10.1016/s1568-2692(02)80030-4
Vago, J. L., Westall, F., Coates, A. J., Jaumann, R., Korablev, O., Ciarletti, V., et al. (2017). Habitability on early mars and the search for biosignatures with the exomars rover. *Astrobiology*, *17*(6–7), 471–510. https://doi.org/10.1089/ast.2016.1533
Van Rijn, L. C. (1984). Sediment transport, part III: Bed forms and alluvial roughness. *Journal of Hydraulic Engineering*, *110*(12), 1733–1754. https://doi.org/10.1061/(asce)0733-9429(1984)110:12(1733)
Vignaga, E., Haynes, H., & Sloan, W. (2012). Quantifying the tensile strength of microbial mats grown over noncohesive sediments. *Biotechnology and Bioengineering*, *109*(5), 1155–1164. https://doi.org/10.1002/bit.24401
Vignaga, E., Sloan, D. M., Luo, X., Haynes, H., Phoenix, V. R., & Sloan, W. T. (2013). Erosion of biofilm-bound fluvial sediments. *Nature Geoscience*, *6*(9), 770–774. https://doi.org/10.1038/ngeo1891
Vignale, F. A., Lencina, A. I., Stepanenko, T. M., Soria, M. N., Saona, L. A., Kurth, D., et al. (2021). Lithifying and non-lithifying microbial ecosystems in the wetlands and salt flats of the central Andes. *Microbial Ecology*, *83*, 1–17. https://doi.org/10.1007/s00248-021-01725-8
Westall, F., Foucher, F., Bost, N., Bertrand, M., Loizeau, D., Vago, J. L., et al. (2015). Biosignatures on mars: What, where, and how? Implications for the search for Martian life. *Astrobiology*, *15*(11), 998–1029. https://doi.org/10.1089/ast.2015.1374
Xuewu, Z., Xin, L., Dexiang, G., Wei, Z., Tong, X., & Yonghong, M. (1996). Rheological models for xanthan gum. *Journal of Food Engineering*, *27*(2), 203–209. https://doi.org/10.1016/0260-8774(94)00092-1
Yallop, M. L., De Winder, B., Paterson, D. M., & Stal, L. J. (1994). Comparative structure, primary production and biogenic stabilization of cohesive and non-cohesive marine sediments inhabited by microphytobenthos. *Estuarine, Coastal and Shelf Science*, *39*(6), 565–582. https://doi.org/10.1016/s0272-7714(06)80010-7